

Characterizing the Large-scale Recovery Capabilities of Atacama Large Aperture Submillimeter Telescope (AtLAST)



Manidipa Banerjee

Université Côte d'Azur

Supervised by:

Dr. Luca Di Mascolo, Kapteyn Astronomical Institute

Dr. Chiara Ferrari, Université Côte d'Azur

Prof. Pasquale Mazzotta, Università degli Studi di Roma "Tor Vergata"



UNIVERSITÉ
CÔTE D'AZUR



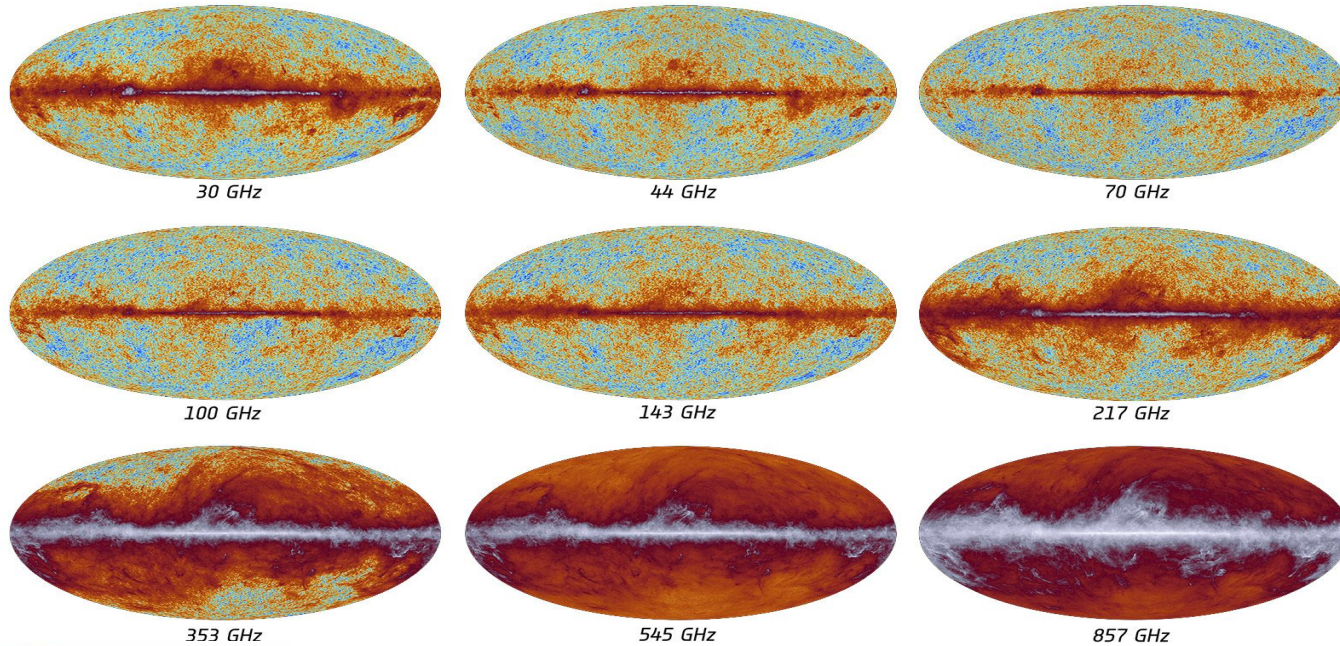
Co-funded by the
European Union

➔ Unveiling the (Sub)-Millimeter Sky



planck

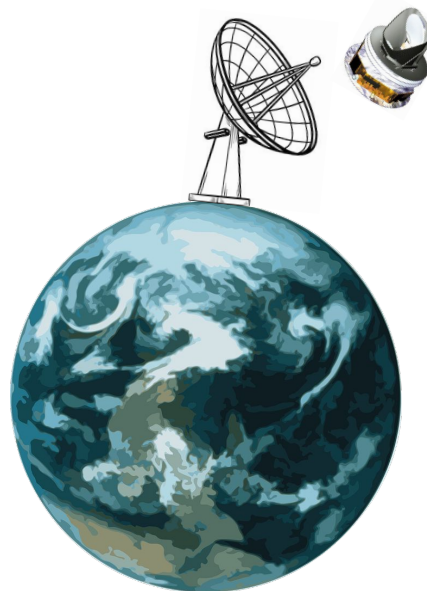
The sky as seen by Planck



➔ Why Need a Single Dish ?



30m telescope - IRAM



Large Single Dish

- Enhances sensitivity to fainter extended emission
- Maximizes sky coverage in a short time



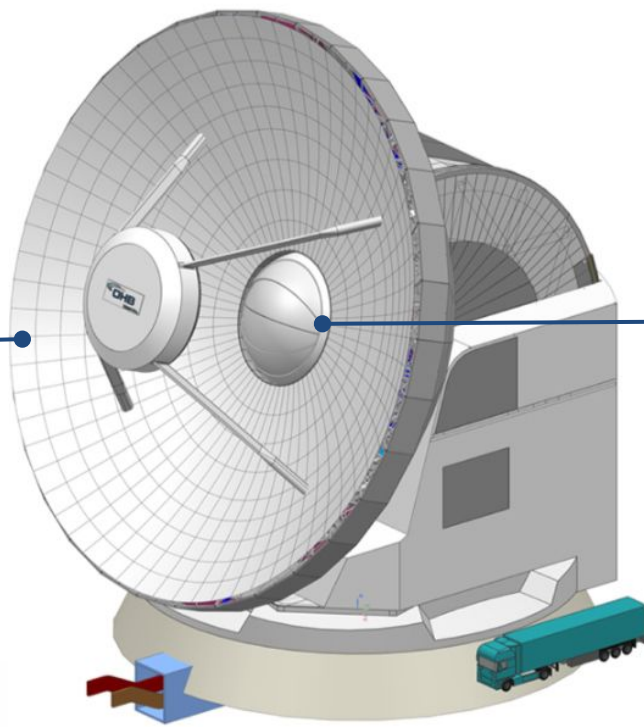
➔ Exploring (Sub)mm Universe with AtLAST

Atacama Large Aperture
Submillimeter Telescope

Site: **Chajnantor Plateau**

Klaassen et al. 2020

Dish diameter: 50 m



Field of View : $1^\circ - 2^\circ$

Fast Scanning Speed !

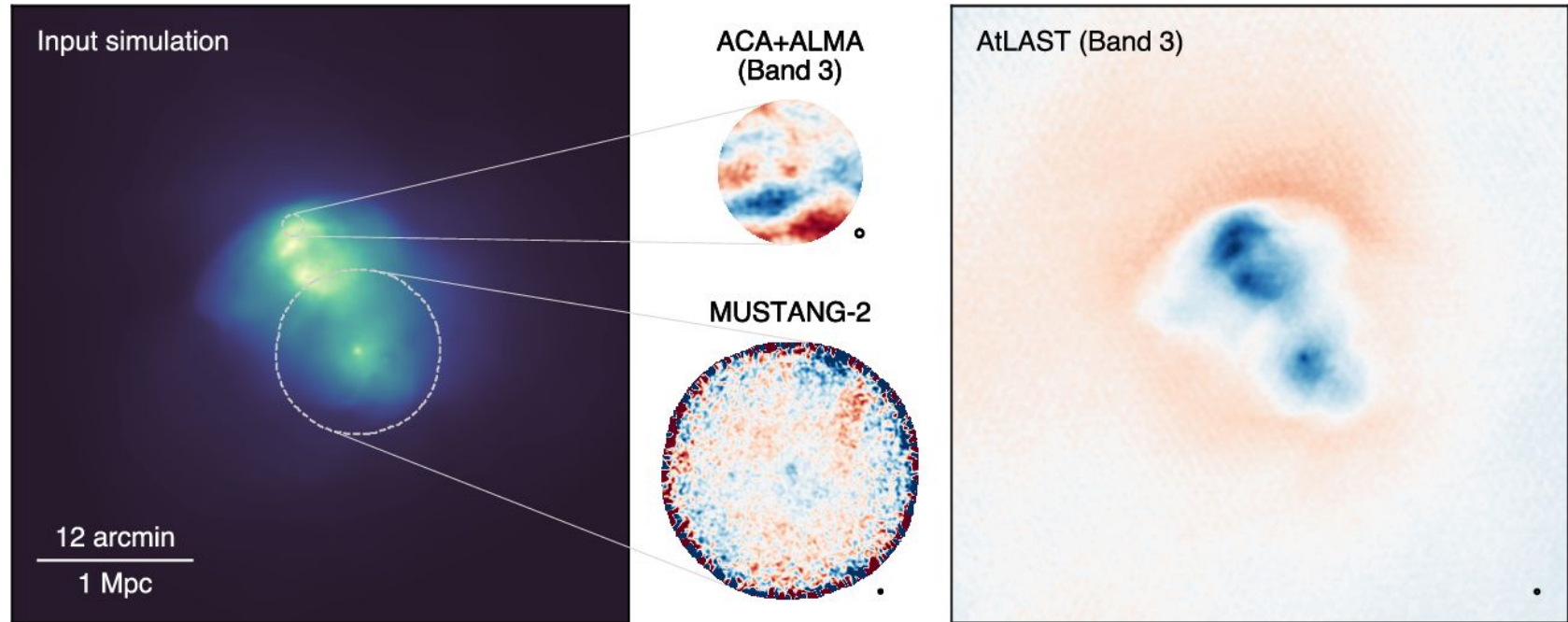
$\sim 3^\circ/\text{s}$

Mroczkowski et al. 2025

AtLAST CAD model (Mroczkowski et al. 2025)



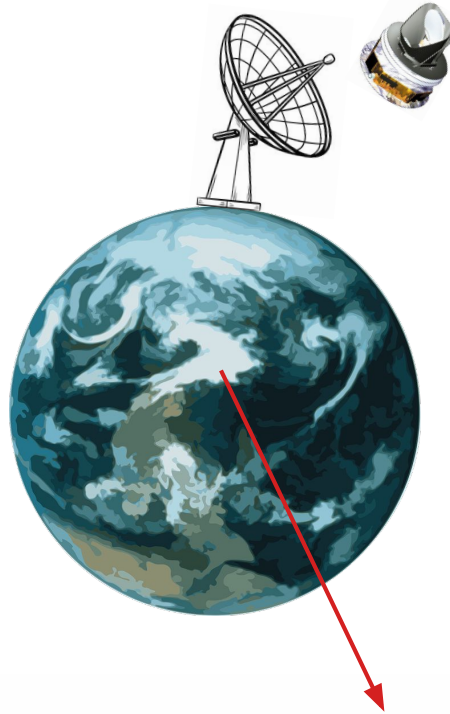
➔ Key Observational Advantage of AtLAST



Di Mascolo et al. 2025



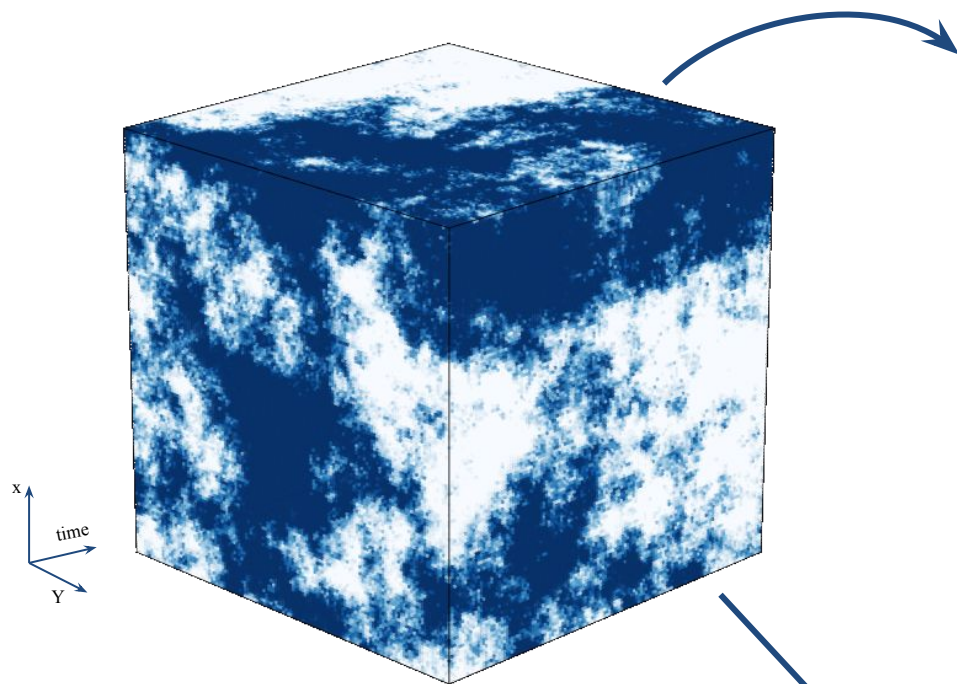
➔ Main Challenge for Ground-based Observations:



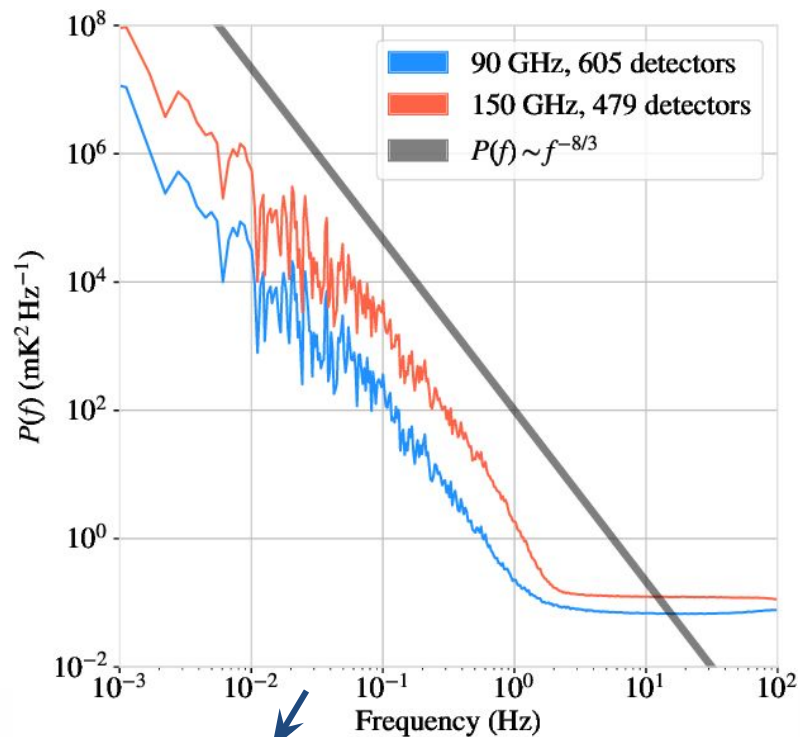
Earth's Atmosphere !



➔ Atmospheric Fluctuations in Ground-Based (Sub)mm Observations



credit: <https://thomaswmorris.com/maria>

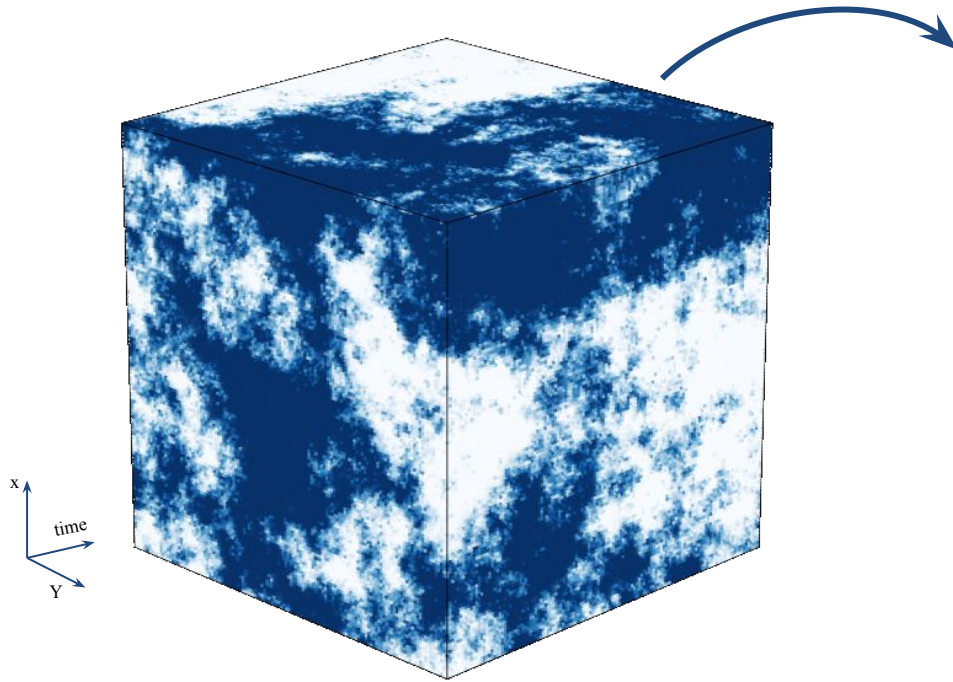


**Large-Scale turbulence evolves
slower than small-scale turbulence.**

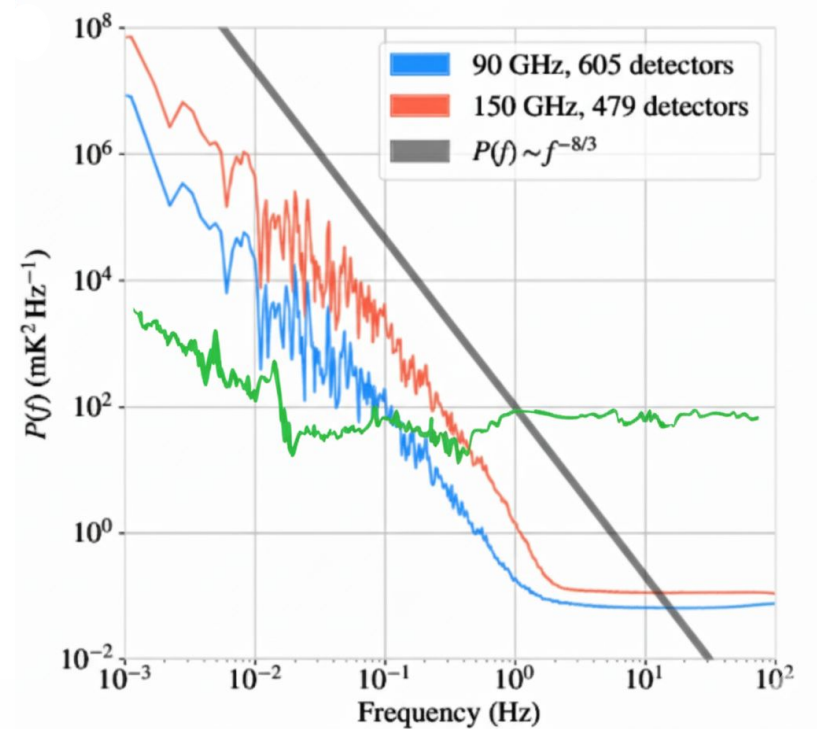
Morris et al. 2022



➔ Atmospheric Fluctuations in Ground-Based (Sub)mm Observations



credit: <https://thomaswmorris.com/maria>

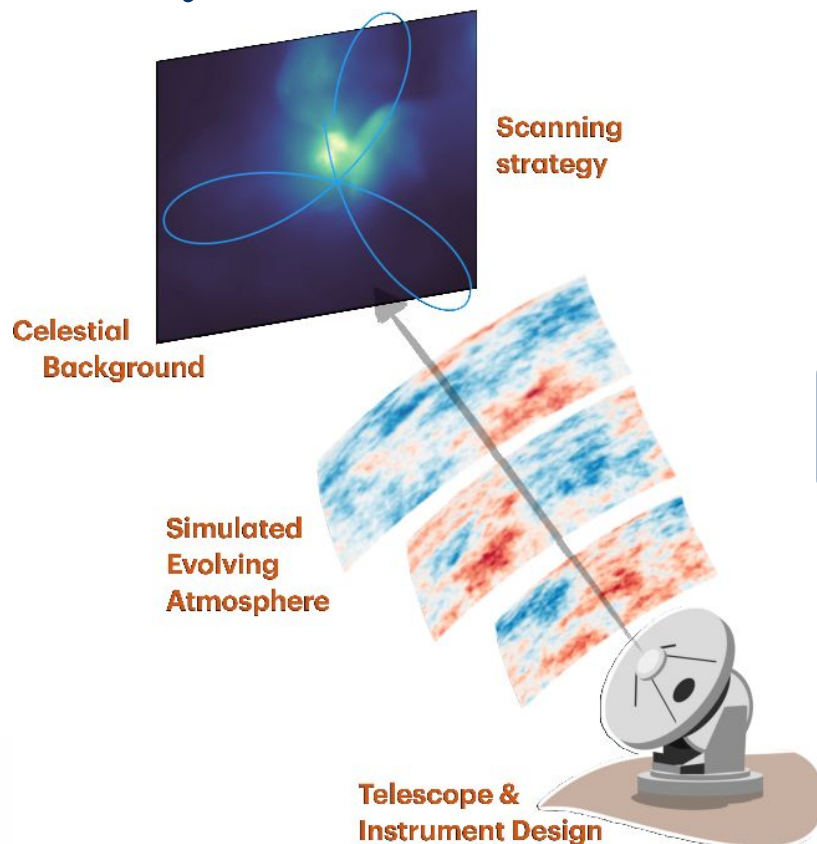


Morris et al. 2022



➔ Motivation: Large-Scale Recovery

- Exploring the ability of such a large aperture single dish telescope to recover extended diffuse emissions under realistic observing conditions.
- Characterizing the impact of different scanning strategies on the telescope's performance in large-scale recovery.



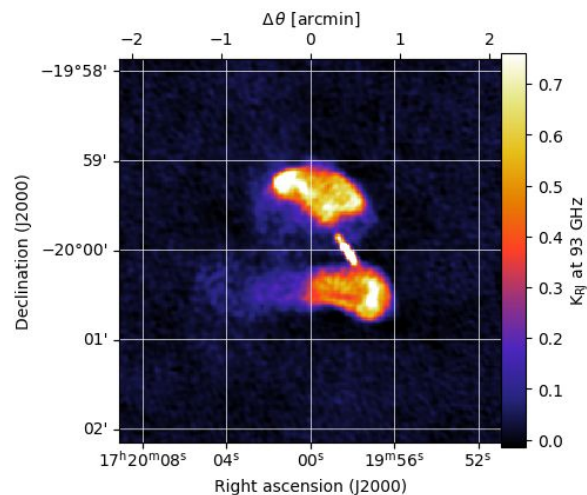
maria
A multipurpose virtual
telescope simulator

Van Marrewijk et al. 2024

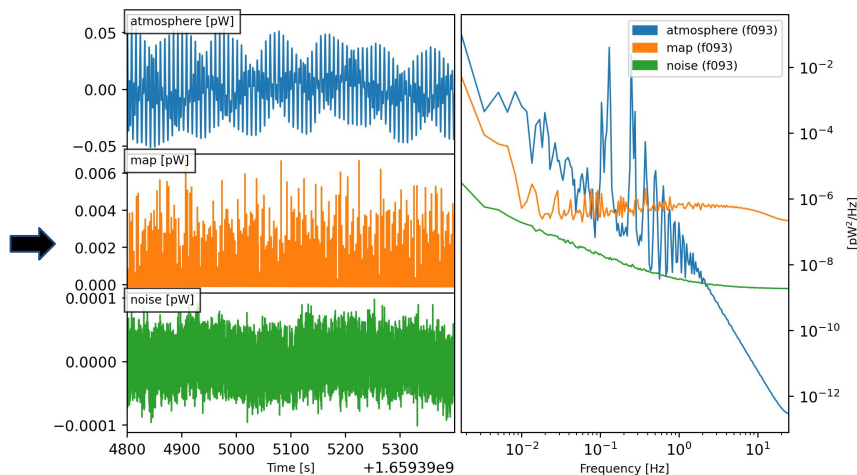
van Marrewijk et al. 2024

➔ Approach: Generating TOD and Output map with maria

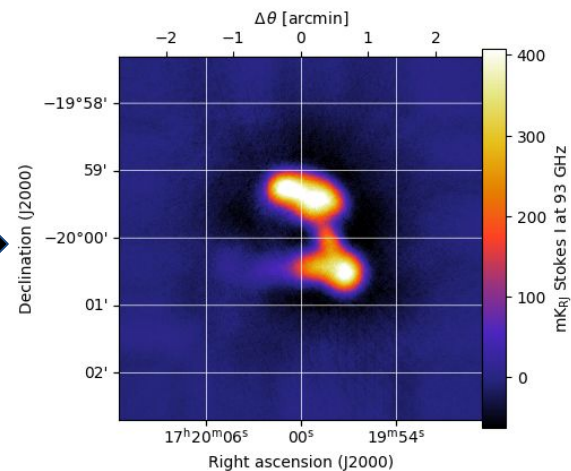
Input map



TOD & Power spectra



Output map



Radio Galaxy 3C288 at $z = 0.246$
(Bridle et al. 1989)

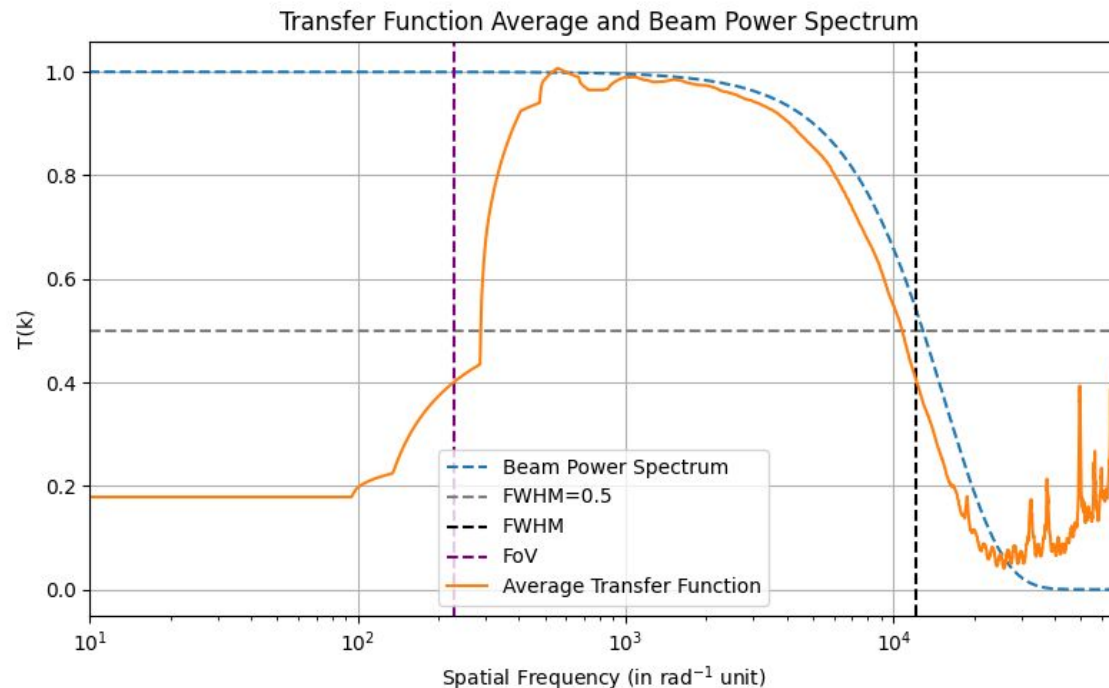


➔ Analysis: Transfer Function Estimation

Transfer function averaged
over atmospheric realizations:

$$\bar{T} = \frac{1}{N} \sum_{k=1}^N \sqrt{\frac{PS_{\text{output}}(k)}{PS_{\text{input}}(k)}}$$

- ➔ $PS_{\text{output}}(k)$ and $PS_{\text{input}}(k)$ are the 1D power spectra of the output and input maps respectively
- ➔ N is the number of atmospheric realizations

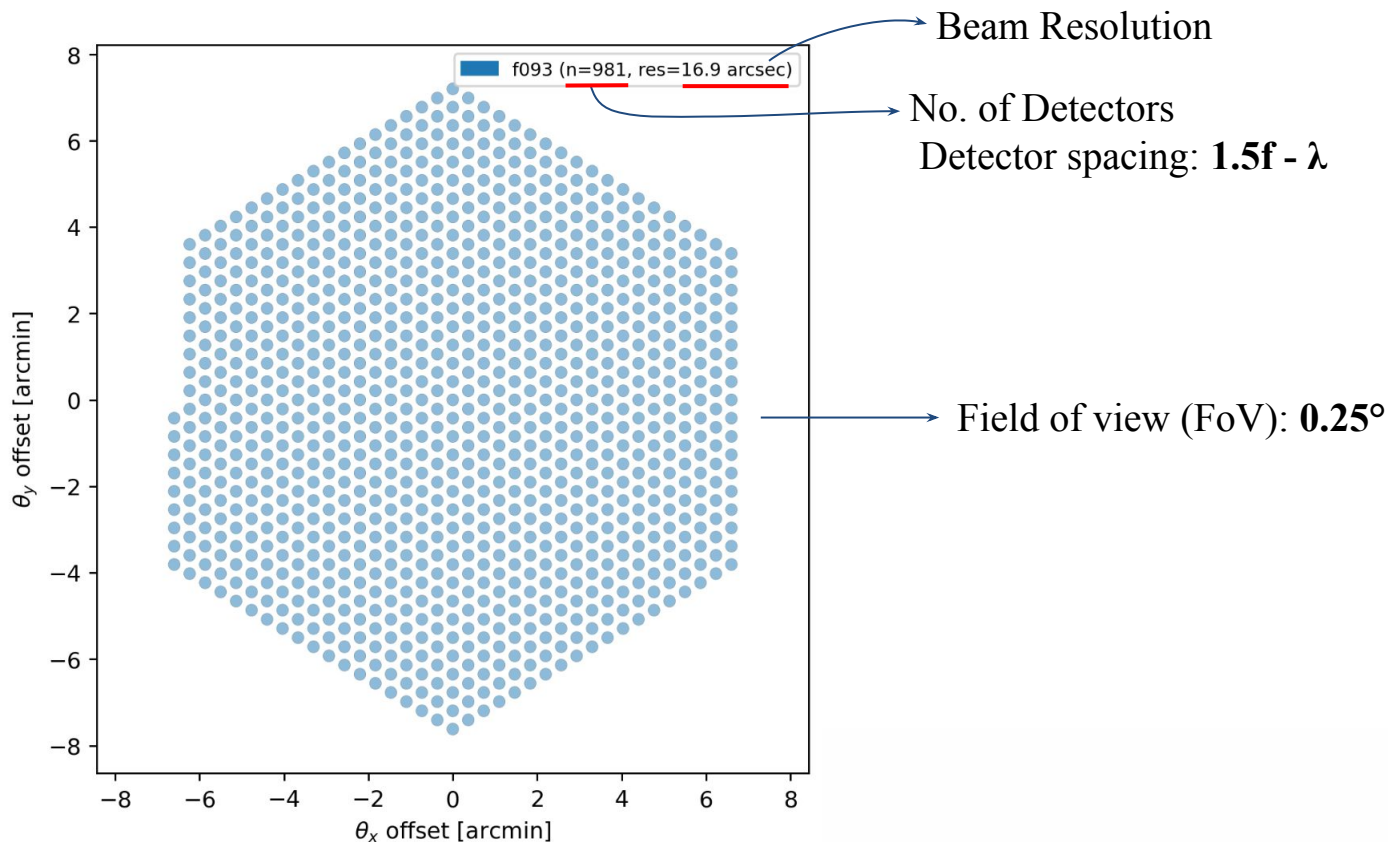


➔ Array Configuration of AtLAST-like Telescope

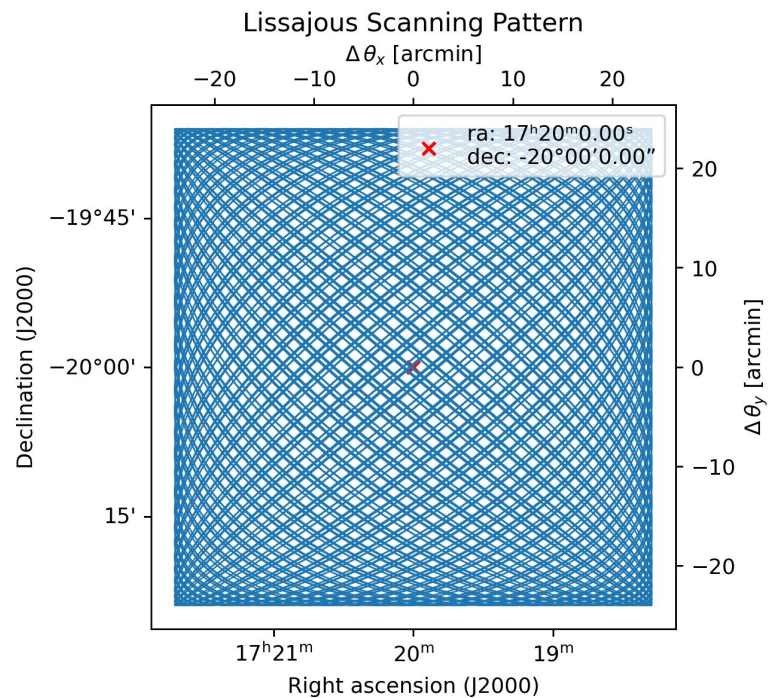
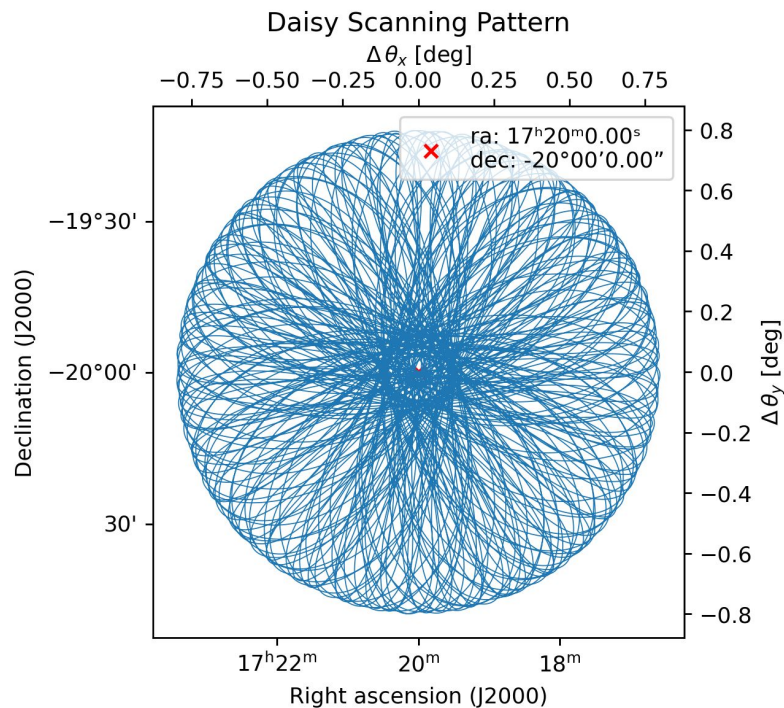
● Observation:

- Observing frequency: **93 GHz**
- Frequency bandwidth: **53 GHz**

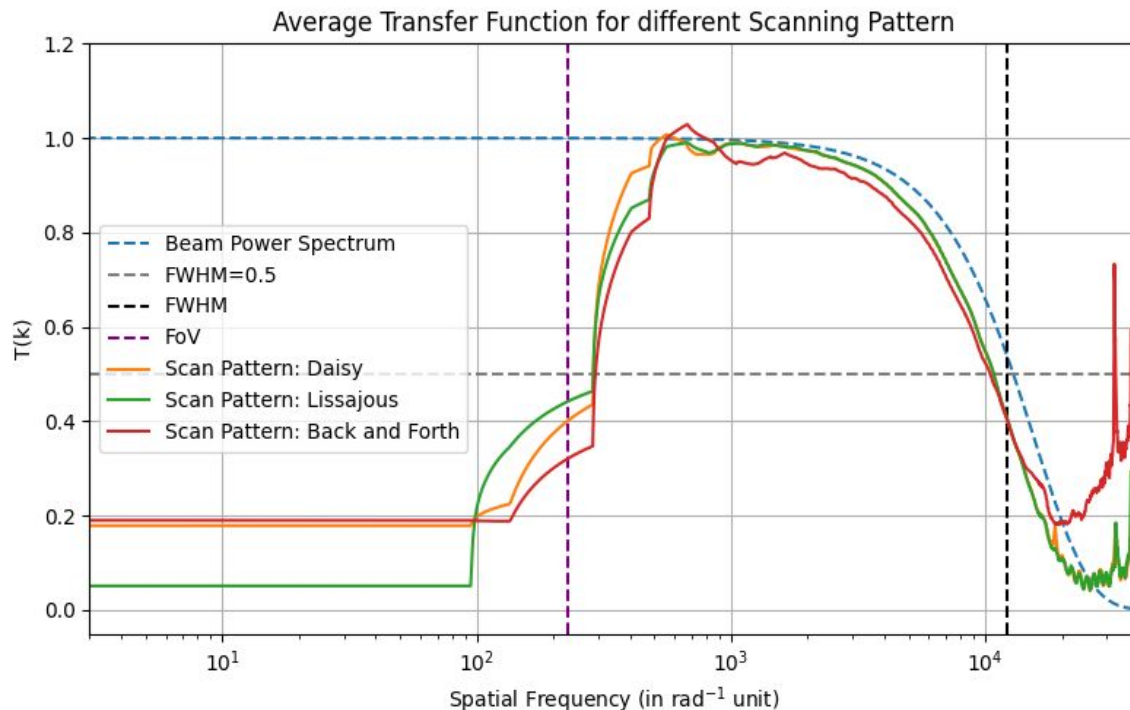
Primary Dish Diameter: **50 m**



➔ How Single-Dish Scans the Sky ?



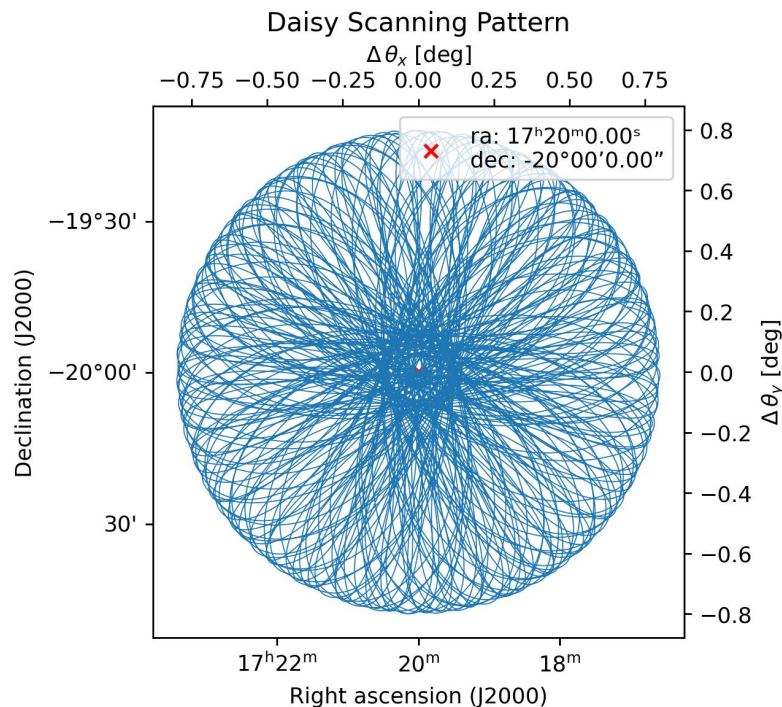
➔ Result: Dependence on Scanning Pattern



- **Minor difference** in corresponding **transfer functions** among these scanning patterns.



➔ Parameters Defining the Scan Strategy

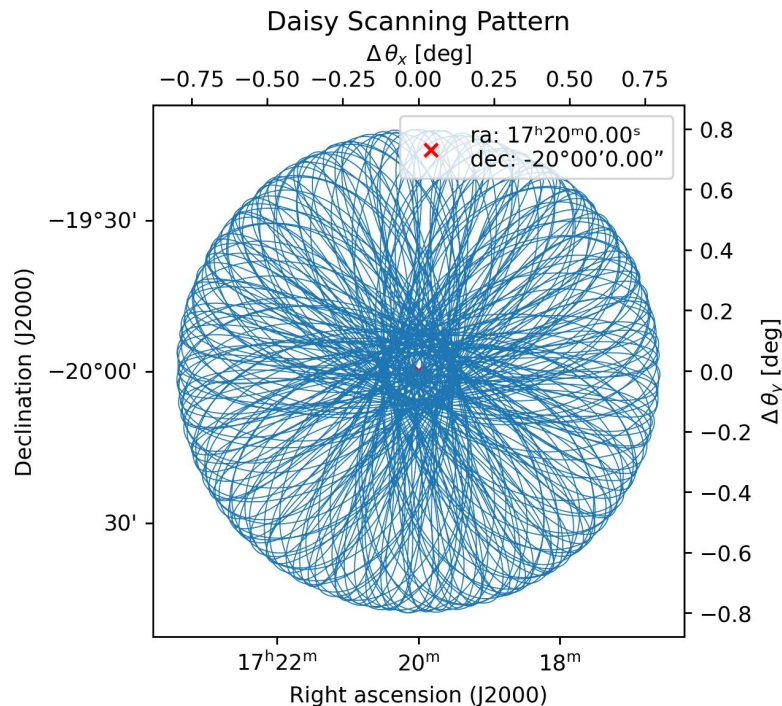


➔ Scanning parameters:

- ◆ Radius
- ◆ Speed
- ◆ Pattern
- ◆ Scan time
- ◆ Sampling Rate



➔ Parameters Defining the Scan Strategy

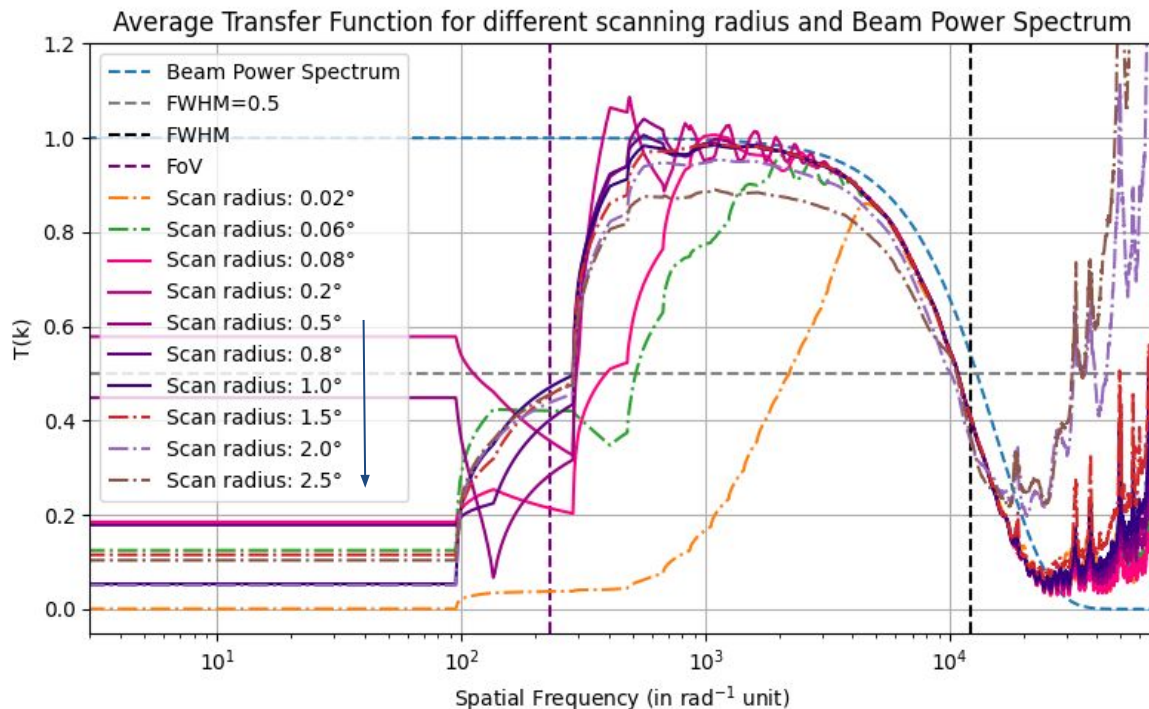


➔ Scanning parameters:

- ◆ **Radius** (0.02° - 2.5°)
- ◆ **Speed** (0.05° s⁻¹ - 4° s⁻¹)
- ◆ Pattern : **Daisy**
- ◆ Scan time : **10 minutes**
- ◆ Sampling Rate : **50 Hz**



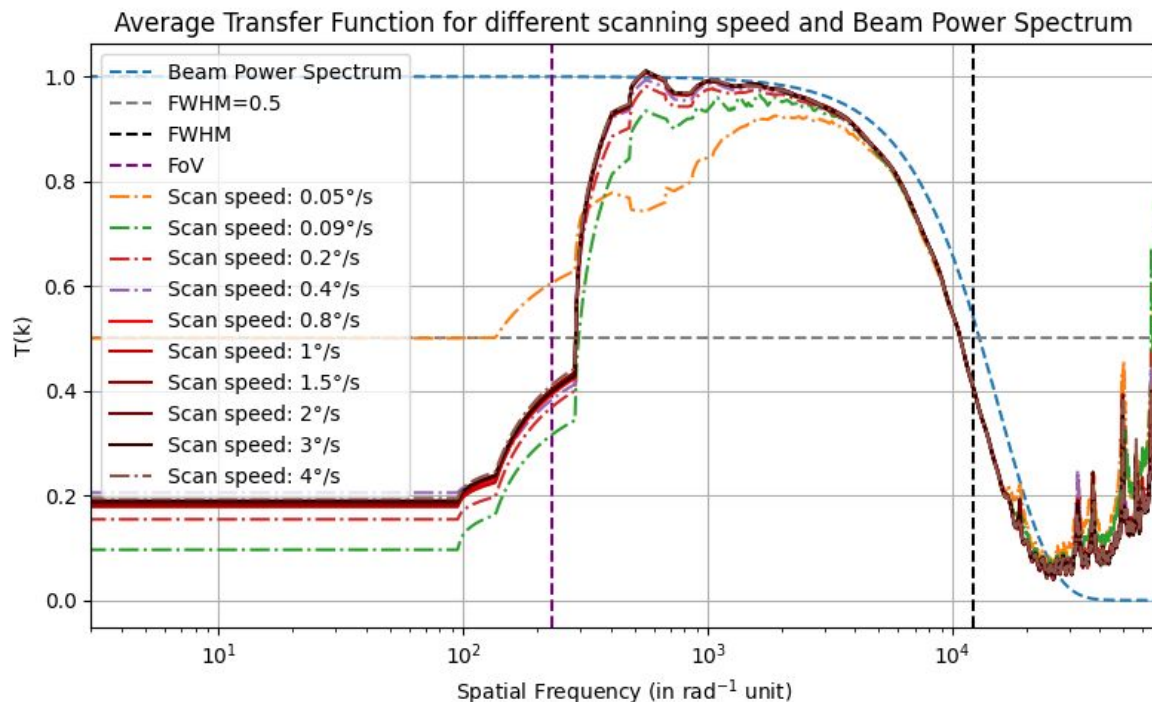
➔ Result: Dependence on Scanning Radius



- At scanning radius $\geq 0.5^\circ$ ($= 2 \times \text{FoV}$), the corresponding transfer functions ~ 1
- Below 0.08° , large-scale modes are filter-out.



➔ Result: Dependence on Scanning Speed



- At scanning speed $\geq 0.8^\circ\text{s}^{-1}$, the corresponding transfer functions ~ 1
- Below 0.09°s^{-1} , large-scale modes are attenuated.



➔ Conclusion & Future Work

- Simulated an **AtLAST-like configuration** to scan the mock sky under realistic observing conditions and therefore reconstructed the sky signal.
- Characterized the telescope performance in **recovering large-scale signal** in (sub)mm regime through transfer function.
- Analysed how the choice of the **observing parameters** i.e. **scan radius**, **scan speed** and **scan pattern** can influence **recovery of fainter extended emission**.
- A potential future extension is to incorporate **full 2° FoV (currently considered 0.25°)**, **multichroic detectors** and **polarization maps**.
- The need for a substantial storage capacity and high-performance computing resources to **reduce the computational time** and support **complex analysis**.
- A quantitative characterization of the **dependence on detector spacing** for a large focal plane array is required for achieving an instantaneous Nyquist sampling.



APPENDIX



➔ Atmospheric Fluctuations at (Sub)mm Wavelengths

Atmospheric Fluctuations (Errard et al. 2015) depend on:

- Wind
- Water vapor
- Turbulence
- Temperature

➔ **Kolmogorov-Taylor Frozen turbulence hypothesis:**

(Kolmogorov, 1941; Taylor, 1938; Morris et al., 2025)

Power spectrum associated
with atmospheric fluctuation

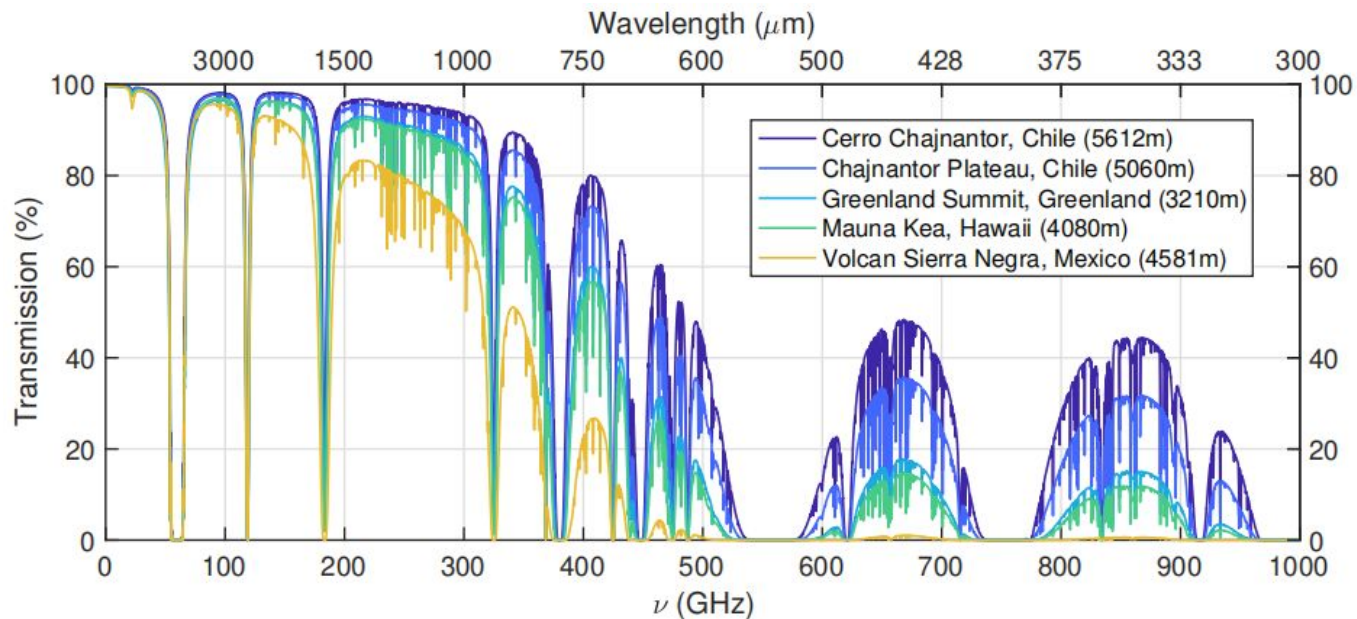
$$P(f) \propto f^{-8/3}$$

Temporal
frequency

- Lower-frequency atmospheric fluctuations contaminate large-scale (sub)mm signals observed by ground-based observatories
- This limitation leads to the requirement of advanced observational strategies to recover large-scale astronomical signals



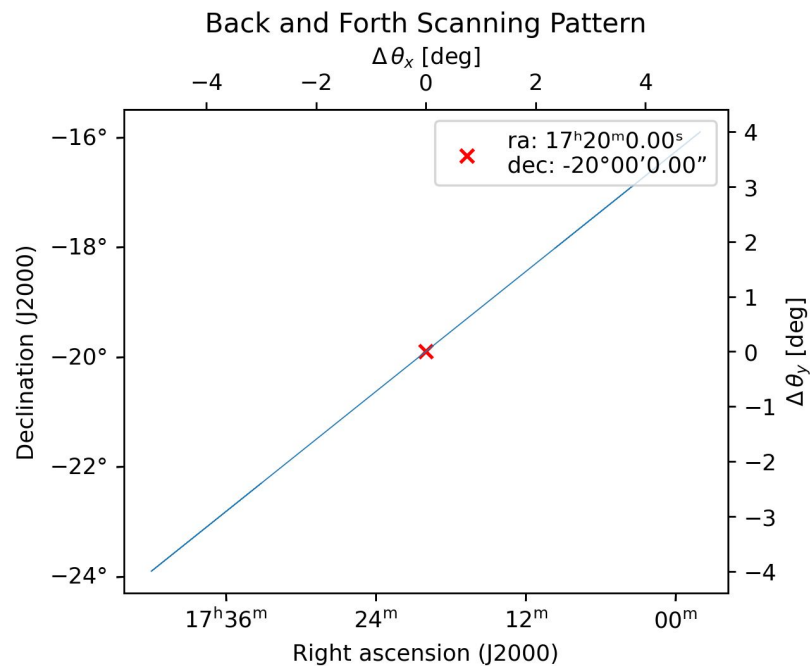
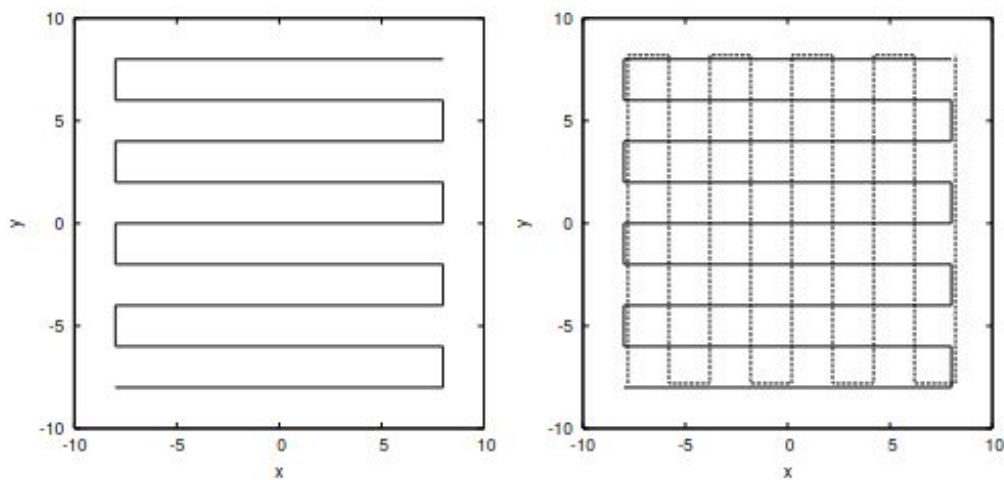
➔ AtLAST's Site on **Llano de Chajnantor Plateau** in Atacama:



Atmospheric transmission at several world-class sites for (sub)mm survey
(Klaassen et al. 2020)



➔ How Single-Dish Scans the Sky ?



➔ How Single-Dish Scans the Sky : Daisy Scan

$$\vec{x}_{\text{outer}} = r_{\text{outer}} \sin(\phi_{\text{outer}}) \exp\left(i \frac{\phi_{\text{outer}}}{n_{\text{petals}}}\right),$$

$$\vec{x}_{\text{inner}} = r_{\text{inner}} \sin\left(\phi_{\text{outer}} + \frac{\pi}{2}\right) \exp\left(i \frac{\phi_{\text{inner}}}{n_{\text{petals}}}\right),$$

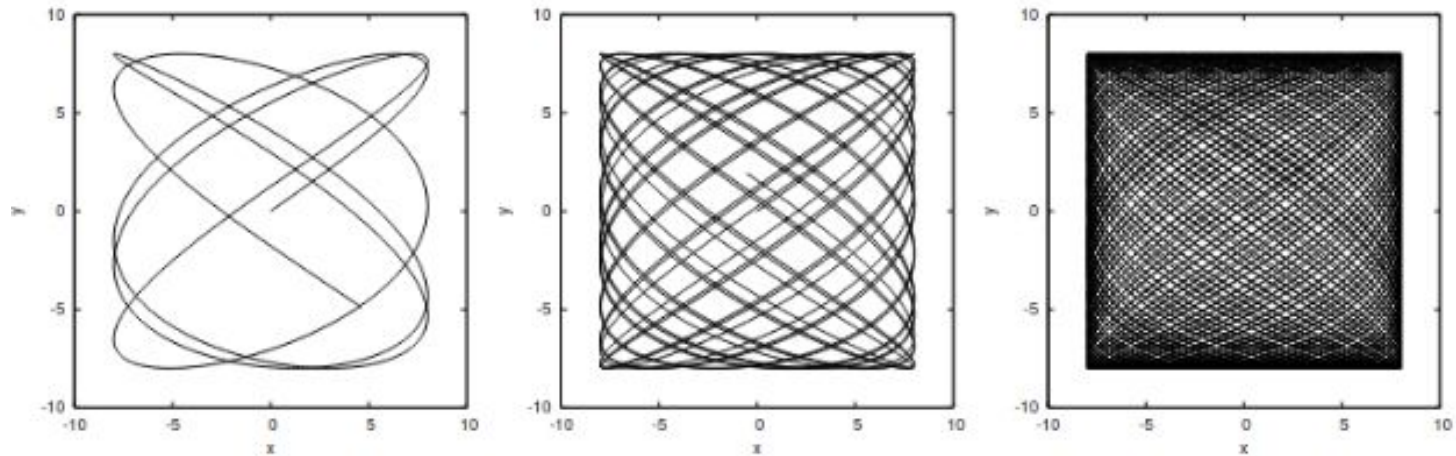
$$\vec{x}_{\text{scan}} = \vec{x}_{\text{outer}} + \vec{x}_{\text{inner}},$$

$$\text{RA, Dec} = \text{Re}[\vec{x}_{\text{scan}}], \text{Im}[\vec{x}_{\text{scan}}],$$

- $r_{\text{inner}} = 0.15 r_{\text{outer}}$
- $\phi_{\text{inner}} = \sqrt{2} \phi_{\text{outer}}$
- $n_{\text{petals}} = 10/\pi$



➔ How Single-Dish Scans the Sky : Lissajous Scan



➔ Maximum Recoverable Scale (MRS)

$$\theta_{\text{MRS}} = \kappa \frac{\lambda}{L_{\text{min}}}$$

$$D_{\text{SD}} \geq \frac{1.18 L_{\text{min}}}{\kappa}$$



Minimum Baseline

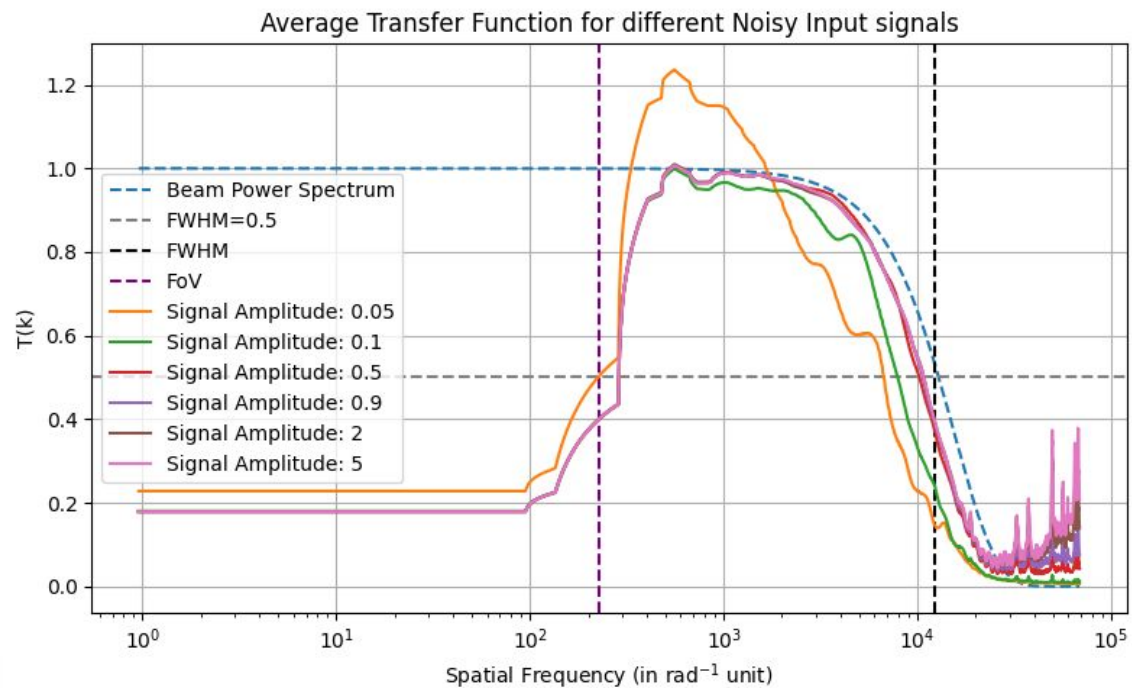


➔ AtLAST Parameters

Parameter	Value
Wavelength (λ) range	0.3–10 mm
Primary mirror diameter	50 m
Field of View (FoV)	2° (1°)
Number of instruments	≥ 5
Scan speed	3°/s
Acceleration	1°/s ²
Elevation (EL) range	20°–90°
Azimuth (AZ) range	$\pm 270^\circ$
Mount type	AZ–EL



➔ Dependence on different Input Signals:



→ Confusion Limit

- The “confusion limit” term refers to a limit within which there are many detected sources in an observation that it is hard to spatially distinguish individual sources apart from each other

- Source distribution in sky fixed
- Gaussian beam

$$\sigma_{\text{conf}} \propto \frac{1}{\theta_0} \longrightarrow \text{FWHM of the beam}$$

Wavelength	ATLAST FWHM (arcsec)	SPIRE FWHM (arcsec)	SPIRE 1σ confusion (mJy)	ATLAST 1σ confusion (mJy)
250 μm	1.26	18.2	5.8	0.40
350 μm	1.76	24.9	6.3	0.45
500 μm	2.52	36.3	6.8	0.47

Table A.1: Comparison of ATLAST vs SPIRE confusion noise across wavelengths

